Applied Thermal Engineering 144 (2018) 804–811

Contents lists available at ScienceDirect

Applied Thermal Engineering

journal homepage: www.elsevier.com/locate/apthermeng

Research Paper

Sustainability evaluation model of geothermal resources in abandoned coal mine

Pingye Guo[a,b], Liange Zheng[c,*], Xiaoming Sun[a,*], Manchao He[a], Yanwei Wang[d], Jingshi Shang[d]

[a] State Key Laboratory for Geo-Mechanics and Deep Underground Engineering, 100083 Beijing, China
[b] School of Mechanics, Architecture and Civil Engineering, China University of Mining and Technology, 100083 Beijing, China
[c] Earth Sciences Division, Lawrence Berkeley National Laboratory, 1 Cyclotron Rd, Mail Stop 90-1116, Berkeley, CA 94709, USA
[d] China Institute of Water Resources and Hydropower Research, 100038 Beijing, China

HIGHLIGHTS

- A sustainability evaluation model of geothermal energy in abandoned coal mine is presented.
- The geothermal potential of abandoned coal mine reservoirs depends on the characteristics of goaf roof.
- The heat extraction rate is related to flow rate, inlet temperature and lifetime.

ARTICLE INFO

Keywords:
Geothermal energy
Abandoned mine
Stope
Sustainability

ABSTRACT

The evaluation of geothermal resource is important for abandoned coal mine reservoir. In this paper, we assessed the geothermal potential of abandoned coal mines using numerical model with key parameters calculated by empirical formula. The volume and spatial distribution of fractures were calculated based on the volume of open space in the abandon mine and strength of roof rock; a 3D model was developed using the MINC method of TOUGH2 simulator. Calculation results show that the geothermal potential of abandoned mine reservoirs depends on not only the permeability of fracture but also the height of fractured zone. Because of the height of fractured zone, the abandoned mine with the strong roof has more geothermal potential than in other cases. Furthermore, sensitivity analyses of key parameters model results indicated that the heat extraction rate is closely related to not only the flow rate but also the injection temperature and lifetime.

1. Introduction

Renewable energy is as one of the environment friendly and sustainable energy options. Low temperature geothermal energy, extracted with heat pump, has been widely used in China for heating and cooling as a clean and economical option. In the meantime, many deep coal-mines in China have been or are about to be closed (for example, eight coal mines have already been closed in Xuzhou city). A great deal of open space is left after mining, which consists of shafts, tunnels and stopes (mined out area). After the mine is decommissioned, this space is filled with water from rainfall, underground aquifers and artificial flooding. Considering the relatively high temperature in deep mines (for example, the abandoned coal mine in Xuzhou at 1000 m deep is over 45 °C), the deep abandoned mines has been considered as good potential low-temperature geothermal reservoirs [1].

The idea of using geothermal energy from mines was proposed as early as in the 1980 s [2]. There have been many cases of using geothermal energy from abandoned mines around the world [3–10]. Despite the great number of successful applications, these projects are usually very small and therefore will not have the problem of heat depletion because the amount of water extracted and used is only a very small portion of the water stored in mine. However, for large-scale projects sustainability is a critical issue because heat resource insufficiency could seriously jeopardize the geothermal utilization project in abandoned mines. Unfortunately, the accurate assessment of heat storage capacity is very challenging for abandoned coalmines because the acquirement of key data about stopes requires field investigation that is costly and time consuming. In this case, numerical model with key data estimated from available field data is a more feasible option to assess the sustainability of geothermal energy of deep abandoned mines.

The heat reservoirs of abandoned mine can be divided into two

* Corresponding authors.
E-mail addresses: lzheng@lbl.gov (L. Zheng), xmcumtb@163.com (X. Sun).

https://doi.org/10.1016/j.applthermaleng.2018.06.070
Received 28 November 2017; Received in revised form 21 June 2018; Accepted 22 June 2018
Available online 23 June 2018
1359-4311/

Nomenclature

T	temperature (°C)
M	mass flow rate (kg/s)
P	pressure (kPa)
Q	rate of heat flow (kW)
Ex	rate of exergy (kW)
H	height (m)
S_f	sagging of the immediate roof
S_{max}	maximum surface subsidence

Subscripts

In	input
out	output
C	caved zone
F	fractured zone

Greek symbols

Λ	bulking factor of rock
ϕ	porosity (%)

types: abandoned tunnels and goafs. The tunnels can be regarded as heat exchangers, and their sustainable geothermal resources can be estimated by a semi-empirical method or simple numerical model [11–16]. The goaf reservoirs are mainly composed of fractures caused by mining whose sustainable geothermal resources are difficult to assess. A more widely used method is to regard the abandoned stopes as an equivalent porous medium [17–23]. In addition to primary porosity, there is secondary porosity in goaf reservoir made by mining, which depends on the mining method and roof conditions. However, the models in the existing literature have rarely considered this issue. Therefore, in this work, taking an abandoned working face as an example, secondary porosity and distributions under different roof conditions are discussed. Meanwhile, a double porous media model that can describe the flow and heat transfer in the fracture of mined out area is established. Moreover, we assumed that the injection well and the extraction well are set at both ends of the working face and that the water was injected into the abandoned mine geothermal reservoir to produce hot fluids for heat pump system (Fig. 1). The effect of injected temperature, flow rate and lifetime on the sustainability is analyzed in different scenarios.

2. Model development

There are two kinds of thermal reservoir in abandoned mines, namely abandoned tunnels and mined out areas. For abandoned tunnel, because of its plenteous data and simple geometry, heat transfer and flow in tunnels can be simulated with a conventional model. However, for the mined-out areas, because of the shortage of necessary data and

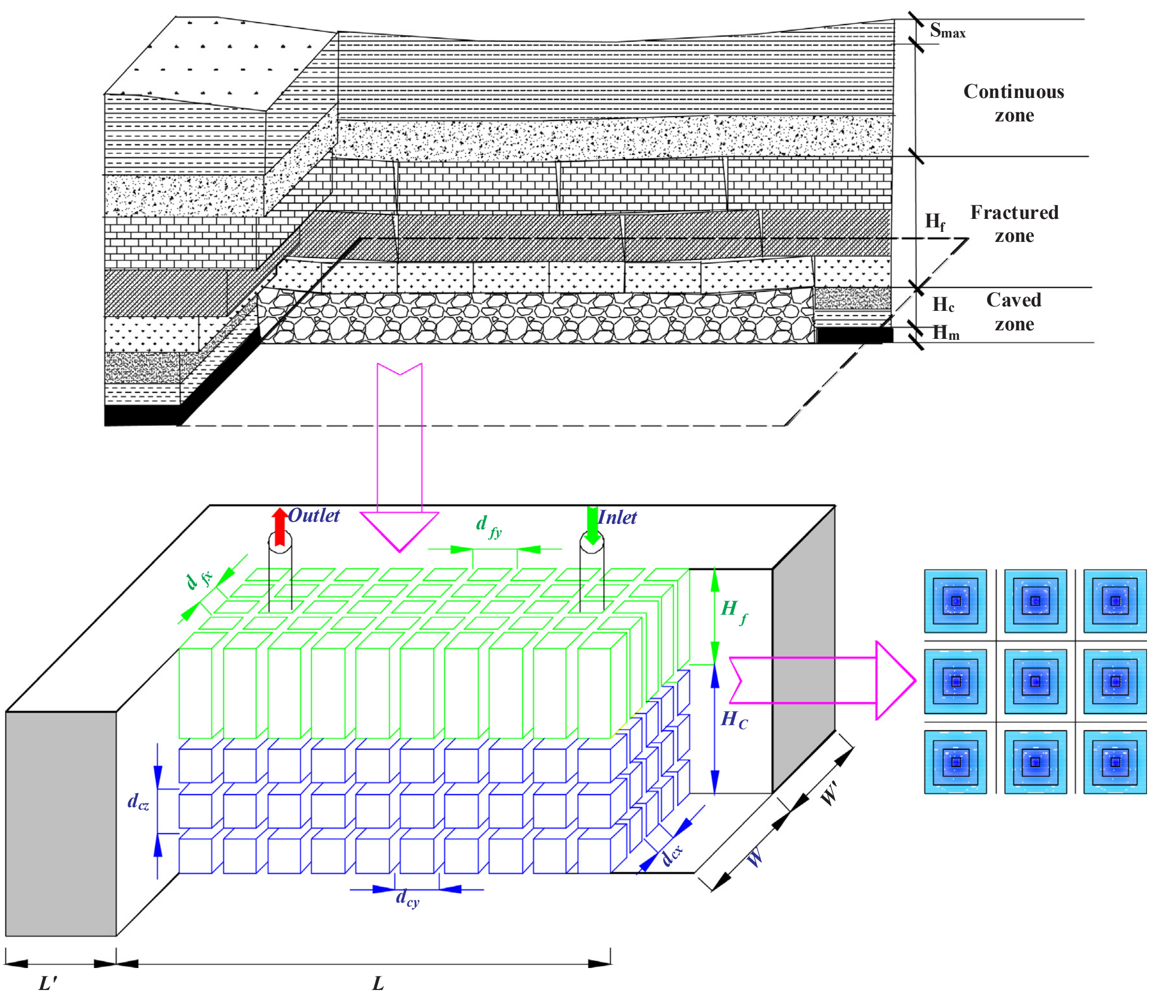

Fig.1. Model of abandoned coal mine workings reservoir.

Table 1
The coefficients with different compressive strength in caved and fractured zone.

ID	Roof rock	Compressive strength (σ_c, MPa)	Coefficients in caved zone			Coefficients in fracture zone		
			c_1	c_2	c	c_1	c_2	c
I	Strong and hard	> 40	2.1	16	2.5	1.2	2.0	8.9
II	Medium strong	20–40	4.7	19	2.2	1.6	3.6	5.6
III	Soft and weak	10–20	6.2	32	1.5	3.1	5.0	4.0
IV	Extremely soft	< 10	7.0	53	1.2	5.0	8.0	3.0

Table 2
Pore characteristic parameter of different roof model.

ID	roof rock	Caved zone			Fractured zone		
		H_c(m)	λ_{cb}	φ_c (%)	H_f(m)	λ_{fb}	φ_f (%)
I	Strong	13.45	1.1159	10.4	53.57	1.0266	2.59
II	Medium strong	9.060	1.1668	14.30	35.72	1.0422	5.0
III	Soft and weak	5.930	1.2559	20.38	20.98	1.0706	6.60
IV	Extremely soft	4.050	1.3770	27.38	13.04	1.1134	10.19

complicated geometry, a new model is needed to calculate the thermal storage capacity. It is very difficult and time-consuming to establish one model that contains the whole mine area. Therefore, it is better to select a typical working face rather than the whole mine for analysis.

2.1. Formation of geothermal reservoir in goafs

Geothermal reservoir in goafs refers to the highly permeable zones formed during mining. As shown in Fig. 1, these highly permeable zones consist of two parts, caved zone and fractured zone. After mining, the rock strata over coal seam will sink due to gravity. After the process of collapsing, breaking, separating, fracturing and bending of rock strata, three different zones will be developed from floor to surface, namely the caved zone, fractured zone and continuous zone. The detailed process is as follows:

First, after the beginning of coal mining, the roof rock begins to move, break and collapse because of gravity until the mined-out space is filled with caved rock because of its bulking. This area is called the caved zone. Due to the strong disturbance of mining, the main features of this area are irregularity, low compactness, and high permeability.

Second, with the advance of mining and time, rock mass overlying roof begins to bend and sink, and a large number of fractures is formed in the upper rock of caved zone. This area is called the fractured zone. With less mining disturbance compared to the caved zone, the fracture distribution in this zone is relatively regular. The direction of fracture is consistent with the normal direction of rock strata. Therefore, this zone demonstrates a higher permeability in the vertical direction than in the horizontal direction.

Last, the rock mass over fractured zone are continuous and elastically deformed. This area is called the bent zone. In general, the effects of mining disturbances are small in the bent zone and few fractures are generated. If the bent zone is composed of weakly permeable rocks such as mudstone, it is an aquifuge, and conversely, it is connected to the thermal reservoir in goafs. In our cases, it is assumed to be an aquifuge. The geothermal reservoirs in goafs refer to the caved and the fractured zone, and which is the focus of this study.

2.2. Calculation method of secondary fracture in goafs

For the abandoned mined area, the porosity of thermal reservoir is partitioned into (1) a primary porosity, which consists of small fractures and pores in the rock matrix, and (2) a secondary porosity, consisting of fractures made by mining. The primary porosity can be measured directly by experiment. However, the secondary porosity is difficult to measure directly. In our study, the secondary porosity was calculated by mining parameters. As shown in the Fig. 1, the volume of secondary porosity can be calculated by volume of mining coal and subsidence [24,25,26]. The height of caved zones and fractured zones can be calculated with empirical formula [26]. The height of caved zone H_c can be expressed as:

$$H_c = \frac{100H_m}{c_1H_m + c_2} \pm c \tag{1}$$

As shown in Table 1, c_1 and c_2 are coefficients depending on the compressive strength of roof rock, and c is a mean square deviation.

For the height of the fractured zone H_f, an empirical formula has been developed from a diverse set of data of mining environment in China with different lithological and mechanical characteristics. And it can be expressed as:

$$H_f = \frac{100H_m}{c_3H_m + c_4} \pm c \tag{2}$$

As shown in Table 2, c_3 and c_4 are coefficients depending on the compressive strength of roof rock mass, and c is also a mean square deviation.

After calculating H_c andH_f , the geometric size of the reservoir is determined. Then, we need to know the total volume and distribution of fractures in the reservoir. To solve this problem, we have to resort to the bulking characteristics of the rock. Bulking is a phenomenon of volume increase that occurs when solid rock is broken [27,28]. The volume of rock may increase when broken because the broken pieces typically do not fit each other perfectly, which results in an increase in void space between rock fragments. Moreover, the secondary porosity

Table 3
Multiple interacting continua (MINC) parameters.

zone	Continuum shell	Thickness (m)	Volume (m^3)	Total volume in grid block (m^3)	Volume fraction (m)
Caved zone	Fracture	0.036	0.104	1.945E + 1	0.104
	Matrix 1	0.042	0.112	2.094E + 1	0.112
	Matrix 2	0.052	0.125	2.338E + 1	0.125
	Matrix 3	0.072	0.150	2.805E + 1	0.150
	Matrix 4	0.798	0.509	9.518E + 1	0.509
	Total	1.000	1.000	1.870E + 2	1.000
Fractured zone	Fracture	0.084	0.025E + 3	1.175E + 1	0.025
	Matrix 1	0.172	0.050E + 3	2.350E + 1	0.050
	Matrix 2	0.462	0.125E + 3	5.875E + 1	0.125
	Matrix 3	1.089	0.250E + 3	1.175E + 1	0.250
	Matrix 4	8.193	0.550E + 3	2.585E + 1	0.550
	Total	10.000	1.000E + 3	4.750E + 2	1.000

Table 4
Fracture permeability of different roof model.

ID	Roof rock	Caved zone		Fractured zone	
		Aperture (m)	Permeability (m^2)	Aperture (m)	Permeability (m^2)
I	Strong	5.49E−04	2.5E−08	1.25E−04	1.3E−09
II	Medium strong	7.71E−04	4.9E−08	1.89E−04	2.9E−09
III	Soft and weak	1.16E−03	1.1E−07	3.14E−04	8.2E−09
IV	Extremely soft	1.63E−03	1.9E−07	4.83E−04	1.9E−08

Table 5
Physical properties parameters of abandoned mine reservoir.

Zone		Density (kg/m^3)	Thermal conductivity (W/m °C)	Heat capacity (J/kg °C)	Porosity (%)	Permeability (m^2)
Cap rock		2650	2.1	900	1	0.1×10^{-16}
Fractured zones	Matrix	2650	2.1	900	5	2×10^{-16}
	Fracture	1500	2.1	900	70	1.3×10^{-09}
Caved zones	Matrix	2650	2.1	900	5	2×10^{-16}
	Fracture	1500	2.1	900	70	2.5×10^{-8}
Base rock		2650	2.1	900	1	0.1×10^{-16}

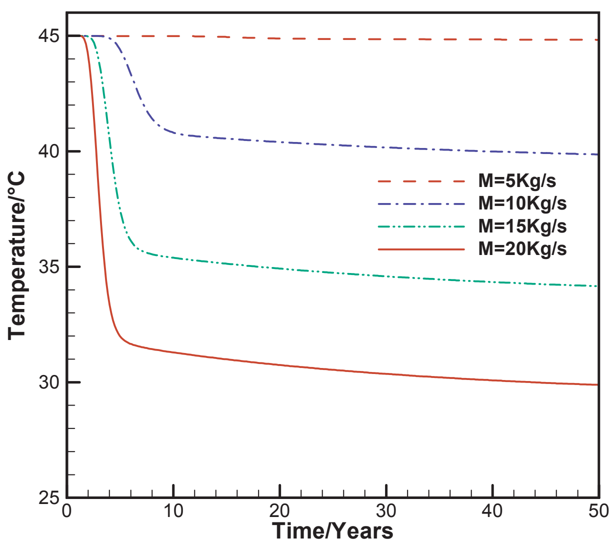

Fig.2. Production temperature with different production mass during the 50 years.

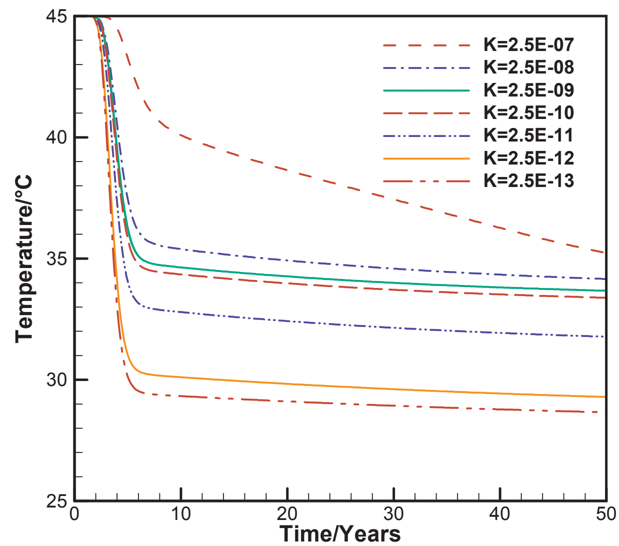

Fig.3. Production temperature with different permeability of fracture.

can be calculated by the bulking factors of rock.

$$\varphi_f = 1 - \frac{1}{\lambda_b} \tag{3}$$

This porosity only refers to the secondary porosity produced by mining. The bulking factor of roof rock λ_b can be derived from the bulking-factor-controlled caving model [29]. In this model, the height of the whole breaking rock including caved and fractured zone can be expressed as:

$$H = \frac{H_m - S_{\max}}{\lambda_b - 1} \tag{4}$$

In Eq. (4), λ_b refers to the bulking factor of whole breaking rock including caved and fractured. Nevertheless, the respective λ_b for the caved and fractured zones are different. Therefore, in our model, it needs to be expressed separately. Theoretically, the height of caved zone can be expressed as

$$H_c = \frac{H_m - S_f}{\lambda_{cb} - 1} \tag{5}$$

In Eq. (5), S_f is the subsidence of fracture zones. Solving equation (5), we can get

$$\lambda_{cb} = \frac{H_m - S_f}{H_c} + 1 \tag{6}$$

For fractured zones, the theoretical height can also be expressed as

$$H_f = \frac{S_f - S_{\max}}{\overline{\lambda_{fb}} - 1} \tag{7}$$

And solving Eq. (7), we could get

$$\overline{\lambda_{fb}} = \frac{S_f - S_{\max}}{H_f} + 1 \tag{8}$$

In Eq. (8), $\overline{\lambda_{fb}}$ is an average value of the fractured zone. In fact, λ_{fb} is a variable from bottom to the top of the fractured zone. According to the experimental results [30], the bulk factor in the fracture zone decreases exponentially with height. It can be expressed as:

$$\lambda_{fb}(h) = \lambda_0 - \varkappa \ln(h + 1) \tag{9}$$

In Eq. (9), $\varkappa$ is the attenuation coefficient. At the bottom of the

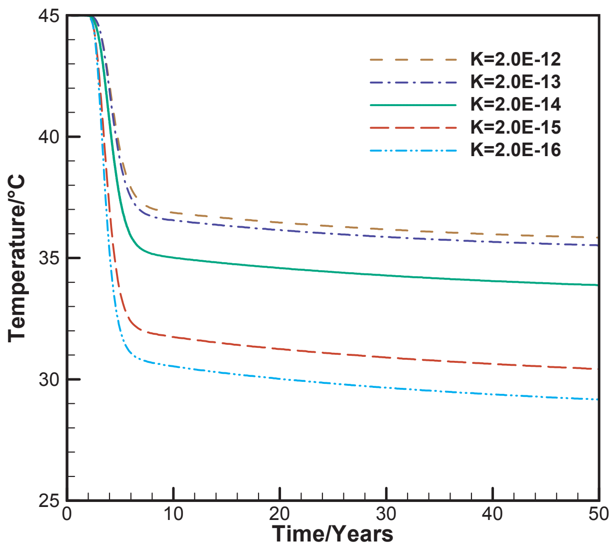

Fig.4. Production temperature with different permeability of roof.

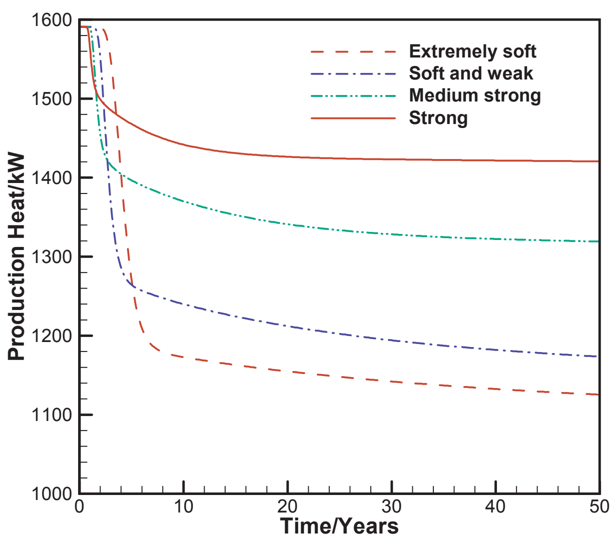

Fig.5. The heat extraction with different roof rock.

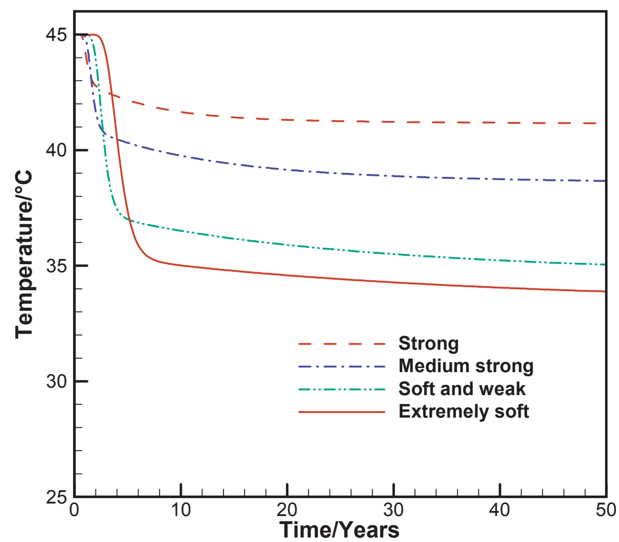

Fig.6. The production temperature with different roof rock and constant permeability.

fractured zones, λ_{fb} equals toλ_{cb}. And at the top of fractured zones, λ_{fb} equals to 1. As a result $\varkappa$ is deduced by

$$\varkappa = \frac{\lambda_{cb}-1}{\ln(H_f+1)} \tag{10}$$

According to Eq. (9) and Eq. (10), the average value of λ_{fb} also can be expressed by:

$$\overline{\lambda_{fb}} = \frac{\int_0^{H_f}\lambda_{fb}(h)dh}{H_f} = 1-\frac{\lambda_{cb}-1}{H_f} + \frac{\lambda_{cb}-1}{\ln(H_f+1)} \tag{11}$$

The combination of Eq. (6), (8), (9) and (11) gives the following expression for the bulking factor calculation:

$$\lambda_{cb} = 1 + \frac{(H_m-S_{\max})\ln(H_f+1)}{H_c\ln(H_f+1)-\ln(H_f+1)+H_f} \tag{12}$$

Insertion of Eq. (11) and (12) into Eq. (3), the porosity produced by mining in the caved zone and the fractured zone can be expressed separately as:

$$\varphi_{cf} = 1-\frac{1}{\lambda_{cb}} \tag{13}$$

$$\varphi_{ff} = 1-\frac{1}{\overline{\lambda_{fb}}} \tag{14}$$

In our study, a 1000 m deep working face was selected in the Jiahe Coal Mine. The working face is 800 m long, 200 m wide and 3 m high. According to the above formula, the development of secondary fractures is closely related to the rock strength of the roof, in addition to the geometry of the working face. Therefore, in this study, we assumed four kinds of roof rock with different strength and calculated the volume of secondary fractures under corresponding conditions. The calculation results are shown in Table 3.

2.3. Numerical model

From the above derivation, it can be concluded that the thermal reservoir in the abandoned mined out area is a dual-porosity medium. Therefore, the dual-porosity multiple interacting continua (MINC) method of TOUGH2 is employed in our model. TOUGH2 is a numerical simulator for non-isothermal flows of multi-component, multiphase fluids in porous and fractured media [31]. It has been used for simulating geothermal systems at many sites [32–35]. Meanwhile, TOUGH2 also provides a multiple interacting continua (MINC) method for simulating fractures [36,37], which is an extension of the classical dual-porosity concept for modeling flow in fractured porous media described by Warren and Root [38]. The survey of geothermal simulations by O'Sullivan et al. [39] showed that the MINC method has been applied at many sites for simulating fracture systems.

For the abandoned coal mine reservoir model, the conceptual model is shown in Fig. 1. It can be divided into three parts, the caved zones, fractured zones and the continuum. First, to reduce the influence of boundary conditions, we suppose that the main reservoirs are surrounded by a large model of continuous media. The main reservoirs include the caved zones which are isotropic and the fractured zones which are anisotropic because the direction of fracture in this region is vertical. For the caved zones, the detailed geometry of the MINC mesh is calculated with the THREE-D proximity function of the MINC preprocessor program of the TOUGH2. For the fracture zones, the detailed geometry of the MINC mesh is calculated with the TWO-D proximity function of the MINC preprocessor program of the TOUGH2. Specific geometric parameters of fracture and matrix MINC grid sub-blocks are shown in Table 3. Moreover, the total volume of the fracture is known, and the permeability can be calculated by cubic law. In the abandoned coal mine reservoir, the volume of fractures is closely related to the

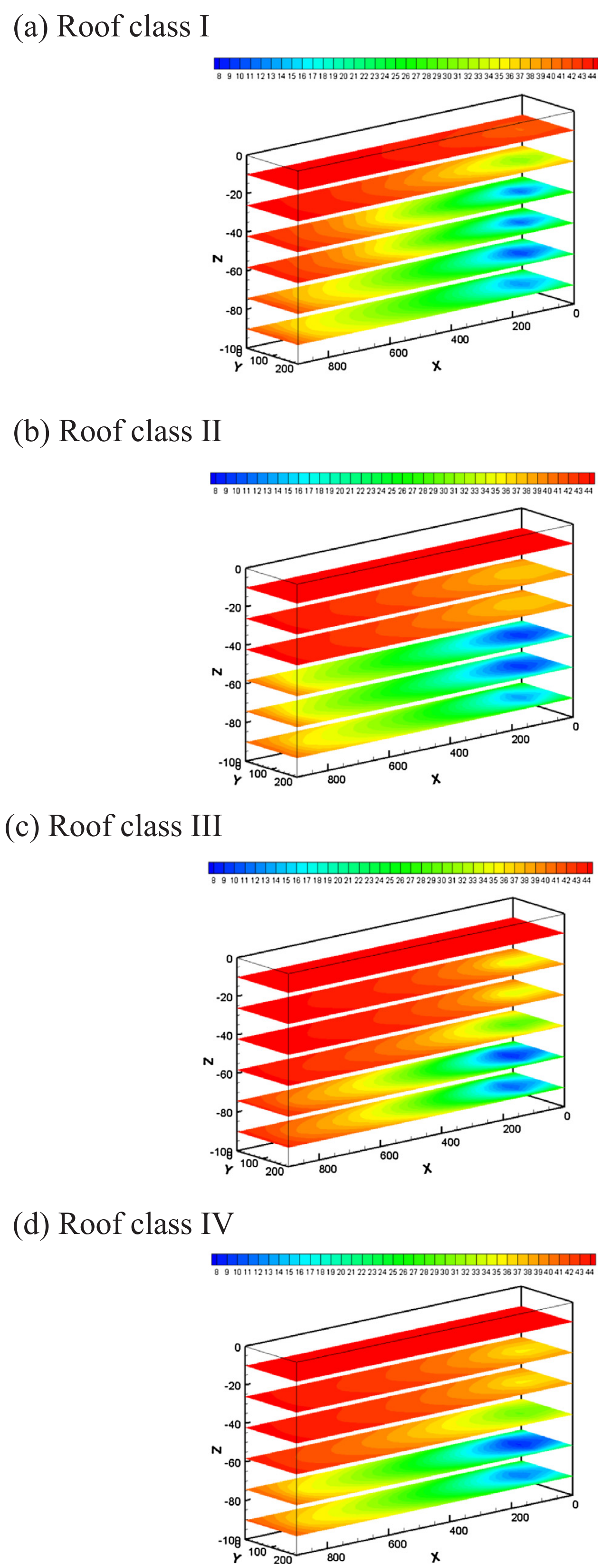

Fig.7. The temperature distribution with different roof rock.

lithology of the roof. In our study, the rock roof is assumed to be divided into four categories according to the strength. The fracture aperture and permeability with different roof were calculated and shown in Table 4.

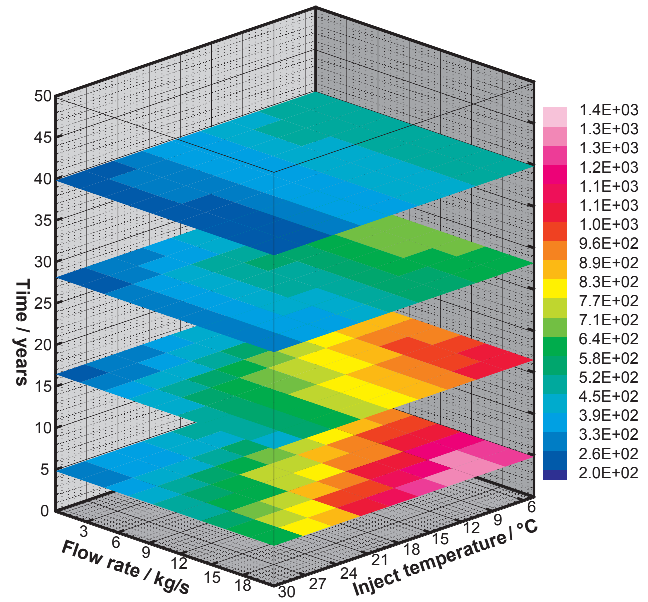

Fig.8. Effect of injected temperature on the production.

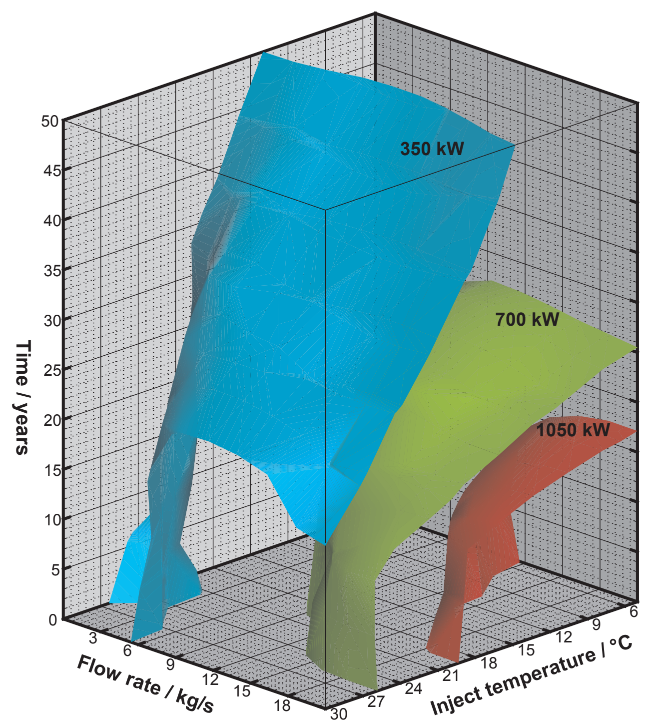

Fig.9. Equal heat extraction rate surface.

3. Results and discussion

In our study, we assumed that the water was injected into the abandoned mine geothermal reservoir to produce hot fluids for heat pump system installed in the ground. First, we discussed the production of heat reservoir with constant injection temperature (8 °C) under strong roof condition. Then, the production and its influencing factors were analyzed under different roof types.

3.1. Effect of flow mass and fracture permeability on heat production

the rock properties used in our model for the strong roof are given in Table 5. Both matrix pores and fractures are assumed to be initially water at a temperature in equilibrium with the surrounding rock, which is 45 °C. The injection and production well are set at both ends of the working face. The results of production temperature with constant injection temperature (8 °C) and different flow rate are presented in Fig. 2. It is shown that the temperature decreases along with the increase of lifetime. At the beginning, the output temperature is 45 °C, which is the same as the initial rock temperature. When the flow rate is 5 kg/s, the production temperature is only slightly lower. However, for the other flow rate, the temperature began to drop soon. After a decade of mining, the decline of temperature slow down because the temperature between production and rock shrinks.

The effect of fracture permeability is important for geothermal reservoir. To investigate the effects of fracture permeability, the simulations were performed for different permeability of fractured zone. The result shown in Fig. 3 indicates that on increasing the permeability from $K = 2.5 \times 10^{-7}$ to $K = 2.5 \times 10^{-13}$, the production temperature decreased. Another important factor is the permeability of roof. Fig. 4 is the production temperature with different permeability of roof rock. It indicates that the permeability of roof rock is beneficial to heat transfer, and the production temperature increases with permeability.

3.2. Effect of different roof rock on heat extraction

The heat extraction rate at 10 kg/s flow rate with different roof are shown in Fig. 5. The result indicates that, from roof Class I to roof Class IV, the sustainable heat production decreases in order. For the roof Class I, the sustainable heat production is 1400 kW, 1300 kW for roof Class II, 1200 kW for the Class III and 1000 kW for roof Class IV. It demonstrates that the height of fractured zone rather than the permeability of fracture has a greater influence on the heat production. From roof Class I to Class IV, though the permeability of fracture increased, the height of fractured zone decreases more. For the roof Class I, the height of fracture zone is 67.02 m, 44.78 m for roof Class II, 26.91 m for roof Class III and only 17.09 m for roof Class IV. It means the greater the strength of the roof rock, the more sparse the fracture distribution, but the wider the spatial distribution of cracks. In order to analyze the effect of fractured height on production temperature, the simulation were performed for different roof type with constant permeability. As shown in Fig. 6, The fractured height of Class I is the highest, and its production temperature is the highest.

The spatial distribution of fractures exerts a great influence on the distribution of temperature. The distribution of temperature in 50 years under the different roof is shown in Fig. 7, where Fig. 7(b) shows the case of roof Class II, Fig. 7(c) shows the case of roof Class III and Fig. 7(d) shows the case of roof Class IV. Comparing the four different cases, it can be clearly seen from Fig. 7 that the greater the rock strength of the roof, the greater the effect of heat extraction on the longitudinal temperature distribution. It is interesting to note that, in the vertical direction, the temperature at -40 m level can reach 10 °C in Fig. 7(a), but only 34 °C in Fig. 7(d). Meanwhile, in the horizontal direction, it is just the opposite situation. This is mainly because the mining fractures in Class I roof reach the -40 m level and those in Class IV do not.

3.3. Effect of different injected temperature on the heat extraction rate

The heat extraction rate depends on not only the flow rate but also the injected temperature. Fig. 8 shows the variation of heat extraction rate at a different flow rate and injection temperatures for a different time. The first conclusion drawn from Fig. 8 is that the effect of flow and injection temperature on heat extraction rate decreases with time. It is obvious that there is no effect of flow rate and very little effect of injecting temperature on heat extraction 20 years later. After 30 years, the heat extraction rate does not increase along with the growth of flow rate, instead the increase of flow rate is counter-productive. It shows that to determine the flow rate we need to consider the time, injected temperature and other factors. In order to choose the optimum extraction time, injection temperature and flow rate, three sets of equal-power surfaces are shown in Fig. 9. If 1000 kW of heat is required, the flow rate and injection temperature must be selected from the red surface. Fig. 9 show the sustainable rate of heat extraction is closely related to the injected temperature, which is the key factor affecting the COP (coefficient of performance) value.

4. Conclusions

This study presents a sustainability evaluation model of geothermal resources in abandoned coal mine. In this model, the volume and spatial distribution of fractures were calculated based on the volume of the mined-out area and the strength of roof rock. Then, a dual porosity numerical model is developed to assess the potential of the reservoir. With model, it is discovered that geothermal potential in abandoned coalmine depends on not only the permeability of fracture but also the height of fractured zone. Because of the higher height of fractured zone, the abandoned mine with the strong roof has more geothermal potential. Another conclusion is that the heat extraction rate depends on not only the flow rate but also the injected temperature and lifetime. In order to improve the heat extraction rate, blindly increase the flow will be counterproductive.

Acknowledgements

Funding for this work was provided by the National Key Research and Development Program (2016YFC0600901), the NSFC (41402273; 41502264) and the Fundamental Research Funds for the Central Universities (2010QL06). The authors wish to thank the reviewers for careful and constructive suggestions.

References

[1] H. Andrew, A.S. John, S. Helen, Geothermal energy recovery from underground mines, Renew. Sustain. Energy Rev. 15 (2011) 916–924.
[2] A.M. Jessop, J.K. Macdonald, H. Spence, Clean energy from abandoned mines at Springhill Nova Scotia, Energy Sources 17 (1995) 93–108.
[3] A.M. Jessop, M.M. Ghomishei, M.J. Drury, Geothermal energy in Canda, Geothermics 20 (1991) 369–386.
[4] G.R. Watzlaf, T.E. Ackman, Underground mine water for heating and cooling using geothermal heat pump system, Mine Water Environ. 25 (2006) 1–14.
[5] S.A. Ghoreishi Madiseh, Mory M. Ghomshei, F.P. Hassani, et al., Sustainable heat extraction from abandoned mine tunnels: a numerical model, J. Renew. Sustain. Energy 4 (2012) 1–16.
[6] J. Raymond, R. Therrien, F. Hassani. Overview of geothermal energy resources in Quebec (Canada) mining environments, in: 10th Int. 'Mine Water Association Congress – Mine Water and the Environment', Karlsbad, Czech Republic, 2008, pp. 99–112.
[7] K. Kathrin, D. Julia, Mine water utilization for geothermal purposes in Freiberg, Germany: determination of hydro geological and thermo physical rock parameters, Mine Water Environ. 29 (2010) 68–76.
[8] M. Preene, P.L. Younger, Can you take the heat?-Geothermal energy in mining, Mining Technol. 123 (2014) 107–118.
[9] D. Banks, A. Fraga Pumar, I. Watson, The operational performance of Scottich mine water-based ground source heat pump systems, Q. J. Eng. Geol. Hydroge. 42 (2009) 347–357.
[10] E.P. Ramos, K. Breede, G. Falcone, Geothermal heat recovery from abandoned mines: a systematic review of projects implemented worldwide and a methodology for screening new projects, Mine Water Environ. 73 (2015) 6783–6795.
[11] R. Rodríguez, M.B. Díaz, Analysis of the utilization of mine galleries as geothermal heat exchangers by means a semi-empirical prediction method, Renew. Energy 34 (2009) 1716–1725.
[12] S.A. Ghoreishi Masiawh, F.P. Hassani, F. Abbasy, Numerical and experimental study of geothermal heat extraction from backfilled mine stopes, Appl. Therm. Eng. 90 (2015) 1119–1130.
[13] J. Raymond, R. Therrien, Low temperature geothermal potential of the flooded Gaspe Mines, Quebec, Canada, Geothermics 37 (2008) 189–210.
[14] J. Raymond, R. Therrien, Optimizing the design of a geothermal district heating and cooling system located at a flooded mine in Canada, Hydrogeol. J. 22 (2014) 217–231.
[15] J. Richardson, D. Lopez, The characterization of flooded abandoned mines in Ohio as a low-temperature geothermal resource. The Geological Society of America, 2016, Special Paper 519.
[16] R.R. Diez, M.B. Diaz-Aguado, Estimating limits for the geothermal energy potential

of abandoned underground coal mines: a simple methodology, Energies 7 (2014) 4241–4260.
[17] V. Hamm, B.B. Sabet, Modelling of fluid flow and heat transfer to assess the geothermal potential of a flooded coal mine in Lorraine France, Geothermics 39 (2010) 177–186.
[18] C. Andres, A. Ordonez, R.A. lvarez, Hydraulic and thermal modeling of an underground mine reservoir, Mine Water Environ. 15 (2015) 1–10.
[19] Z. Malolepszy, Modeling of geothermal resources within abandoned coal mines, Upper Silesia, Poland. in: Geothermal Training Programme 1998, Orkustofnun, Grensasvegur 9, IS-108 Reykjavik, Iceland.
[20] Z. Malolepszy, Low temperature, man-made geothermal reservoirs in abandoned workings of underground mines, in: Proceedings, Twenty-Eighth Workshop on Geothermal Reservoir Engineering, 2003, SGP-TR-173.
[21] C. Loredo, N. Roqueni, A. Ordonez, Modelling flow and heat transfer in flooded mines for geothermal energy use: a review, Int. J. Coal Geol. 4 (2016).
[22] A. Renz, H.J.G. Diersch, Numerical modeling of geothermal use of mine water: challenges and examples, Mine Water Environ. 28 (2009) 2–14.
[23] J. Uhlik, Jan Baier, Model evaluation of thermal energy potential of hydrogeological structures with flooded mines, Mine Water Environ. 31 (2012) 179–191.
[24] V. Palchik, Formation of fractured zones in overburden due to longwall mining, Environ. Geol. 44 (2003) 28–38.
[25] V. Palchik, Experimental investigation of apertures of mining-induced horizontal fractures, Int. J. Rock Mech. Min. Sci 47 (2010) 502–508.
[26] V. Palchik, Bulking factors and extents of caved zones in weathered overburden of shallow abandoned underground workings, Int. J. Rock Mech. Min. Sci. 79 (2015) 227–240.
[27] State Coal Industry Bureau, Order of Coal Pillar Preserving and Pressure of Coal Mining for Coal Under Buildings, Rivers and Railway Lines, Coal Industry Press, Beijing, 2002 (in Chinese).
[28] M. Bai, F. Kendorski, D. Roosendaal Van, Chinese and North American high-extraction underground coal mining strata behavior and water protection experience and guidelines.in: Proceedings of the 14th International Conference on Ground Control in Mining, Morgantown, 1995, pp. 209–217.
[29] H. Yavuz, An estimation method for cover pressure re-establishment distance and pressure distribution in the goaf of longwall coal mines, Int J. Rock Mech. Min. Sci. 41 (2004) 193–205.
[30] S.S. Peng, H.S. Chiang, Longwall Mining, Wiley, New York, 1984, p. 708.
[31] K.Zh. Deng, M. Zhou, Zh.X. Tan, et al., Study on laws of rockmass breaking induced by mining, J. China U. Min. Technol. 27 (1998) 260–264.
[32] K. Pruess, C. Oldenburg, G. Moridis, TOUGH2 User's Guide, Version2. Lawrence Berkeley National Laboratory, LBNL-43134, 2011 (revised).
[33] T. Xu, Y. Ontoy, P. Molling, N. Spycher, M. Parini, K. Pruess, Reactive transport modeling of injection well scaling and acidizing at Tiwi Field Philippines, Geothermics 33 (2004) 477–491.
[34] P.F. Dobson, S. Salah, N. Spycher, E.L. Sonnenthal, Simulation of water-rock interaction in the Yellowstone geothermal system using TOUGHREACT, Geothermics 33 (2004) 493–502.
[35] Hyung-Mok Kim, Jonny Retqvist, et al., Exploring the concept of compressed air energy storage (CAES) in lined rock caverns at shallow depth: a modeling study of air tightness and energy balance, Appl. Energy 92 (2012) 653–667.
[36] K. Pruess, T.N. Narasimhan, On fluid reserves and the production of superheated steam from fractured vapor dominated geothermal reservoirs, J. Geophy. Res. 87 (1982) 9329–9339.
[37] K. Pruess, T.N. Narasimhan, A practical method for modeling fluid and heat flow in fractured porous media, Soc. Petro. Eng. J. 2 (1985) 14–26.
[38] J.E. Warren, P.J. Root, The behavior of naturally fractured reservoir, Soci. Petro. Eng. 228 (1963) 245–255.
[39] M.J. O'Sullivan, K. Pruess, M.J. Lippmann, State of the art of geothermal reservoir simulation, Geothermics 30 (2001) 395–429.